Multiple Ionization of Atoms in Intense Laser Fields

A. Rudenko, C. D. Schröter, R. Moshammer, K. Zrost, V. L. B. de Jesus, B. Feuerstein, D. Fischer, T. Ferger and J. Ullrich

Max-Planck-Institut für Kernphysik, D-69117 Heidelberg, Germany

Abstract. A new ultrahigh vacuum-compatible ($\sim 10^{-11}$ mbar) "reaction microscope" was built to investigate multiple ionization of atoms and molecules in ultra-short (23 fs), intense laser pulses ($10^{14} - 10^{16}$ W/cm^2, 795 nm) . In first experiments ion momentum distributions for single and double ionization of noble gas atoms in the nonsequential and sequential intensity regime were measured using linearly polarized laser pulses. The apparatus is currently improved to perform measurements under even lower residual gas pressures ($< 10^{-13}$ mbar). Furthermore, the new apparatus is ideally suited for future studies on dissociation and Coulomb explosion of molecules.

INTRODUCTION

In recent years experimental and theoretical work has concentrated on multiple ionization by short intense laser pulses (for recent reviews see [1, 2]). Experimental imaging techniques [3, 4], combined with latest progress in laser development, lead to a new generation of differential measurements. Recent investigations on helium [5], neon [6], and argon [7] succeeded in measuring momentum distributions of the doubly and triply charged ions at intensities where nonsequential multiple ionization dominates the total ion yield (intermediate intensity regime of $\sim 10^{14}$ W/cm^2). At present it is generally accepted that the so-called 'rescattering' scenario is the dominant nonsequential double-ionization mechanism. Since ion-momentum distributions alone do not give complete information about the underlying dynamics during recollision, the interest focused on the correlation between the electrons emitted by an atom in the intense laser field. Using a kinematical analysis of two-electron momentum correlation patterns for the nonsequential double ionization in Ar, Feuerstein et al. [8] succeeded in separating two different double-ionization mechanisms. Both are based on the recollision of the first ionized electron with its parent ion core. In addition to the (e,2e) mechanism they identified excitation of the parent ion during recollision with subsequent tunnel ionization of the excited electron as a second important mechanism. Thus, in order to study the dynamics of electron recollision in the presence of the laser field, e.g. the intensity or pulse-time dependence, kinematically complete experiments are called for.

To perform such experiments a new ultrahigh vacuum (UHV)-compatible "reaction microscope" was built (residual gas pressure of $\sim 10^{-11}$ mbar). With this apparatus, which combines recoil-ion and many-electron momentum spectroscopy, first kinematically complete measurements on argon are currently performed. The spectrometer is equipped with large-area position-sensitive detectors (ø 127 mm for ion detection) and therefore ideally suited for studies on dissociation and Coulomb explosion of molecules.

EXPERIMENTAL SET-UP

The new "reaction microscope" is based on a well localized, low-density (10^8 atoms/cm^3), inherently cold atomic target being realized by a supersonic expansion (for reviews on cold-target recoil-ion momentum spectroscopy (COLTRIMS) see [3, 4]). The target for the first experiment was formed by expanding Ar gas at a pressure of 3 bar through a 30 μm nozzle. The inner jet fraction passes through two skimmers with diameters of 200 and 400 μm, respectively. After expansion, the beam is collimated over a total length of 2.1 m to a diameter of 400 μm at the center of an UHV-chamber. The chamber, containing the spectrometer and two position-sensitive multi-channel plate (MCP) detectors, is pumped by turbomolecular and additional volume getter pumps, which results in a residual gas pressure of $3 \cdot 10^{-11}$ mbar.

The experiments were performed using linearly polarized light pulses of a Kerr-lens mode locked Ti:sapphire laser at 795 nm wavelength amplified to pulse energies of up to 350 μJ at 3 kHz repetition rate. The light pulses of 23 fs (FWHM) are focused by a spherical on-axis mirror (f = 100 mm) on the gas jet target. The focal diameter is about 7 μm, which has been determined from measured optical parameters of the laser beam. Ions created in the laser focus are accelerated by a weak homogeneous electric field of 1 V/cm onto a large MCP detector (ø 127 mm, 100 μm position resolution). The electric field is generated by means of 30 cylindrical aluminium electrodes, which are gold plated to ensure for a homogeneous work function. The ejected electrons are registered by a second position-sensitive MCP detector (ø 86 mm) placed opposite to the ion detector. A superimposed homogenous magnetic field (8 Gauss) confines the electron trajectories [11]. From the time-of-flights and the positions of impact on the detectors the charge state and the momentum vector of the ion as well as the momentum vectors of the electrons can be determined.

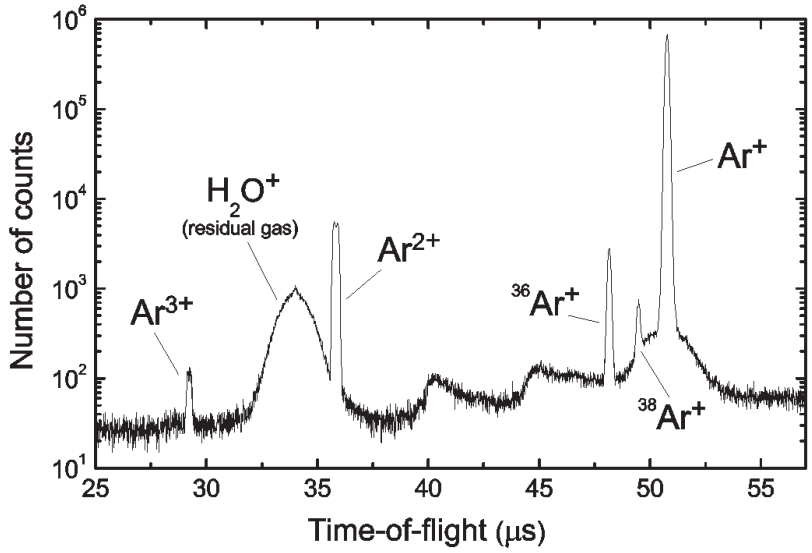

FIGURE 1. Time-of-flight distribution for Ar ions (laser peak intensity 0.5 PW/cm^2).

A typical time-of-flight (TOF) spectrum of argon ions is shown in figure 1. Besides of target specific TOF-peaks a broad background contribution due to ionization of water

molecules from the residual gas is still observed. Because these residual gas ions hit the detector at a different position than those emerging from the jet-target this background can easily be subtracted by placing appropriate conditions on the position spectrum.

RESULTS

Longitudinal momentum distributions of ions (i.e. the ion momentum component parallel to the polarization axis) have been measured for single, double and triple ionization of Ar by linearly polarized laser pulses at a peak intensity of 0.5 PW/cm^2 (figure 2). The light polarization direction was parallel to the spectrometer axis resulting in a momentum resolution of better than 0.1 a.u..

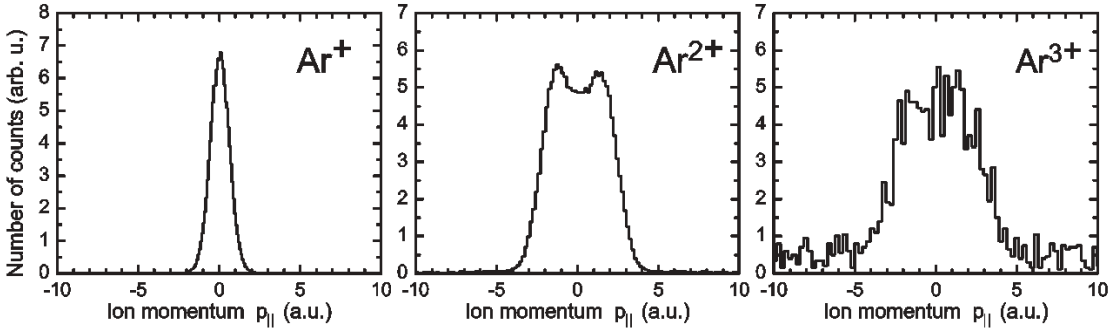

FIGURE 2. Longitudinal momentum spectra for Ar^+, Ar^{2+} and Ar^{3+} ions (laser intensity 0.5 PW/cm^2).

The actual laser intensity was determined by analyzing the single ionization electron spectrum in comparison with the ADK tunneling theory (for details see [9]). The accuracy of this method for absolute intensity calibration is estimated to be better than 15 %. Intensity fluctuations were monitored during the experiment and kept below 10 %. The laser intensity of 0.5 PW/cm^2 corresponds to a Keldysh parameter of $\gamma = 0.51$ indicating that the production of singly charged ions occurs mainly via tunnel ionization. Since the ions are created at a phase where the field strength and, thus, the tunneling probability maximizes, the ions gain only a very little drift momentum in the laser field and hence the momentum distribution peaks at zero. In contrast, the Ar^{2+} distribution shows a double-hump structure with symmetric peaks at ± 2 a.u. and a minimum at zero momentum. As already discussed in previous publications (see e.g. [10]) this double-hump structure is a clear signature of electron rescattering. There the doubly charged ion is produced when the first ionized electron recollides with its parent ion and knocks out a second electron in an (e,2e)-like collision. Since this most likely occurs at an instant when the electric field of the light wave is close to a zero crossing, the ion acquires a large drift momentum. A similar scenario, i.e. an electron impact induced double ionization event during recollision, could explain the production of triply ionized Ar. Based on the ion momentum distribution alone, however, a definite statement about the triple ionization mechanism is not possible. This will be a subject of future investigations.

Figure 3 summarizes the longitudinal ion momentum spectra for He^{2+}, Ne^{2+} and Ar^{2+} measured at different intensities in the range from 0.08 up to 2.2 PW/cm^2. If direct electron-impact ionization during rescattering is the dominant process then the

kinetic electron energy of the returning electron in relation to the ionization potential of the parent ion is a decisive parameter. Therefore, we compare the three ion species at intensities corresponding for each row to almost the same maximum recollision energy, i.e. $E_{max} = 3.17 \cdot U_p$, in units of the ionization potential I_p^+ of the singly charged ion. The numbers on the right of each spectrum indicate this ratio E_{max} / I_p^+, while the numbers on the left give the laser intensity in PW/cm^2. The laser intensities range from the multiphoton regime (Ar^+ at 0.08 PW/cm^2), over the nonsequential up to the sequential regime, which is achieved for Ne and Ar at the highest measured intensities, respectively. With higher laser intensity the ponderomotive potential U_p increases and the ion drift momentum is getting larger. As a result broader momentum distributions are observed.

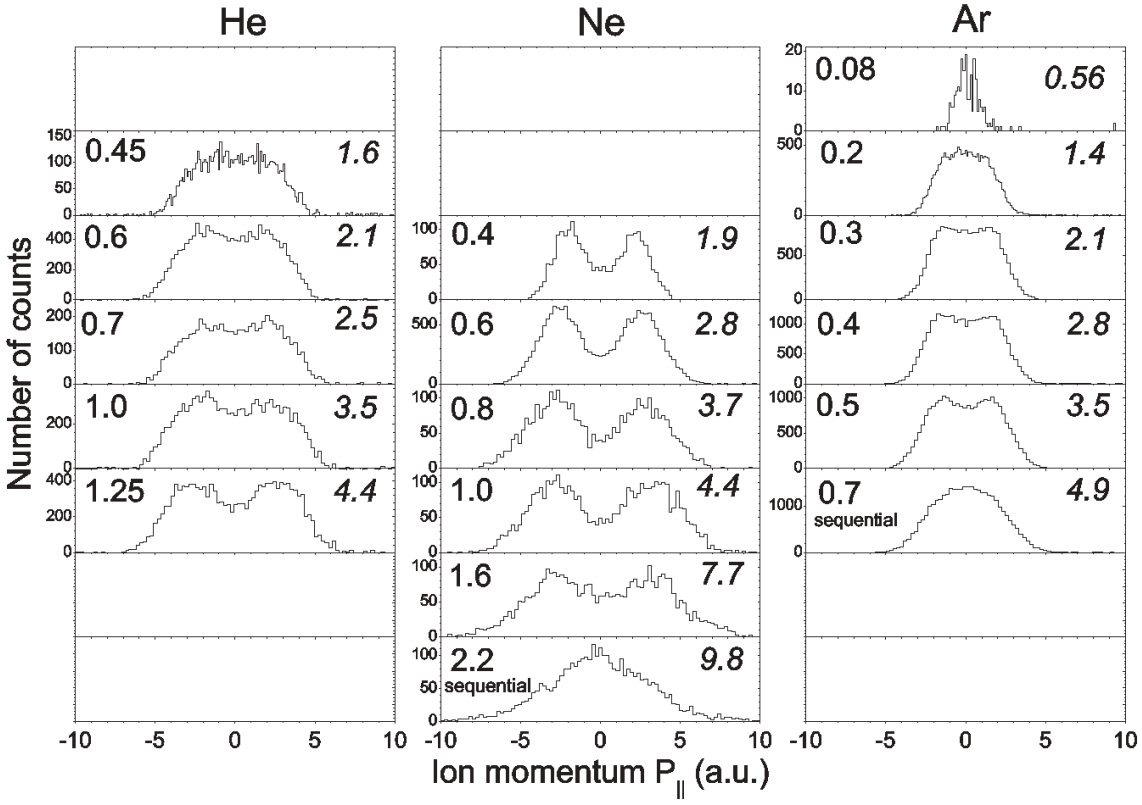

FIGURE 3. Longitudinal momentum spectra for He^{2+}, Ne^{2+} and Ar^{2+} ions at different laser intensities given in PW/cm^2 by the numbers on the left of each spectrum. For the numbers on the right see text.

A qualitative difference in shape and intensity dependence of the momentum spectra of the doubly charged ions is observed for Ne compared to He and Ar, which behave similarly. The shape of the spectra for Ne shows only a weak intensity dependence with a pronounced double-hump structure. A clear transition from a single maximum to a broad structure is observed for He and Ar. In order to explain these qualitative differences we estimated the relative contributions of direct ionization and excitation-tunneling during rescattering based on field-free electron impact cross sections for ionization and excitation [9]. It turned out that for He and Ar excitation during recollision followed by subsequent field ionization is the dominant nonsequential ionization mechanism over

a wide intensity range, while direct (e,2e) ionization dominates in Ne. Hence, even at this high laser intensities the atomic structure determines the nonsequential ionization pathways.

ACKNOWLEDGMENTS

This work was partially supported by the Deutsche Forschungsgemeinschaft within the Leibniz-program. Financial support by the BMBF under contract 05 KS1EB1/2 is gratefully acknowledged.

REFERENCES

1. Protopapas M., Keitel C. H. and Knight P. L., *Rep. Prog. Phys.* **60**, 389-486 (1997).
2. Dörner R., Weber Th., Weckenbrock M., Staudte A., Hattass M., Schmidt-Böcking H., Moshammer R. and Ullrich J., *Adv. At. Mol. Opt. Phys.* **48**, 1-34 (2002).
3. Ullrich J., Moshammer R., Dörner R., Jagutzki O., Mergel V., Schmidt-Böcking H. and Spielberger L., *J. Phys. B: At. Mol. Opt. Phys.* **30**, 2917-2974 (1997).
4. Dörner R., Mergel V., Jagutzki O., Spielberger L., Ullrich J., Moshammer R., Schmidt-Böcking H., *Phys. Rep.* **330**, 95-192 (2000).
5. Weber Th., Weckenbrock M., Staudte A., Spielberger L., Jagutzki O., Mergel V., Afaneh F., Urbasch G., Vollmer M., Giessen H. and Dörner R., *Phys. Rev. Lett.* **84**, 443-446 (2000).
6. Moshammer R., Feuerstein B., Schmitt W., Dorn A., Schröter C. D., Ullrich J., Rottke H., Trump C., Wittmann M., Korn G., Hoffmann K. and Sandner W., *Phys. Rev. Lett.* **84**, 447-450 (2000).
7. Weber Th., Weckenbrock M., Staudte A., Spielberger L., Jagutzki O., Mergel V., Afaneh F., Urbasch G., Vollmer M., Giessen H. and Dörner R., *J. Phys. B: At. Mol. Opt. Phys.* **33**, L127-L133 (2000).
8. Feuerstein B., Moshammer R., Fischer D., Dorn A., Schröter C. D., Deipenwisch J., Crespo Lopez-Urrutia J. R., Höhr C., Neumayer P., Ullrich J., Rottke H., Trump C., Wittmann M., Korn G. and Sandner W., *Phys. Rev. Lett.* **87**, 043003 1-4 (2001).
9. de Jesus V. L. B., Feuerstein B., Zrost K., Fischer D., Rudenko A., Afaneh F., Schröter C. D., Moshammer R. and Ullrich J., *submitted to Phys. Rev. Lett.*
10. Feuerstein B., Moshammer R. and Ullrich J., *J. Phys. B: At. Mol. Opt. Phys.* **33**, L823-L830 (2000).
11. Moshammer R., Unverzagt M., Schmitt W., Ullrich J. and Schmidt-Böcking H., *Nucl. Instrum. Meth.* B **108**, 425-445 (1996).